JOURNAL OF MATERIALS SCIENCE 33 (1998) 763–768

Directional solidification and magnetic properties of MnSb–Sb eutectic composite

Y. PAN, G. X. SUN
Department of Mechanical Engineering, Southeast University, Nanjing 210018, People's Republic of China

The microstructures, solidification behaviour, crystal orientation and magnetic properties of MnSb–Sb eutectic with a high entropy of solution have been studied systematically. The present approach reveals the inherent correlations between them. MnSb–Sb eutectic is characterized by a non-faceted–non-faceted type of growth and well-distributed aligned MnSb rods embedded in a Sb matrix on a micron scale, an ideal composite structure, during directional solidification. The scaling laws of the variation in interrod spacing λ (or rod diameter d) with growth velocity are quantitatively developed. A parallel orientation relation between [001] of MnSb and rod axis is identified through electron diffraction patterns, indicating that the highly anisotropic composite has been fabricated successfully. The hysteresis loops of directionally solidified MnSb–Sb composites are determined along the MnSb rod axis. The saturation magnetization and constant permeability have been evaluated by considering the alignment, size and magnetocrystalline anisotropy.

1. Introduction

The first-row transition-metal antimonides, which all have the NiAs structure, show a large variety of magnetic properties. While MnSb is the only ferromagnetic compound, CrSb, FeSb and CoSb are antiferromagnetic compounds, TiSb is paramagnetic and NiSb is diamagnetic [1]. MnSb is of particular interest as a magnetic material because of its very high axial magnetic anisotropy and the easy direction of magnetization as a function of the temperature [2–4]. The multicomponents consisting of MnSb and other components with different physical properties will make up a functional composite which has become of great importance both theoretically and for industrial applications.

The MnSb–Sb composite will be expected to possess unique magnetic properties if the diamagnetic antimony provides a good dispersion medium for MnSb magnetic fibres by means of directional solidification. On the other hand, the Sb–Mn alloy is also a unique system for investigating the effect of solidification-induced microstructural changes on magnetic properties because of eutectic morphology as a function of the entropy of solution, ΔS_α, and the volume fraction of the minor phase, V_f [5]. The outstanding characteristics of the system are that ΔS_α for the intermetallic compound MnSb has not been reported in the literature and ΔS_α of the matrix Sb is approximately $22\,J\,K^{-1}\,mol^{-1}$ near to a ΔS_α value of $23\,J\,K^{-1}\,mol^{-1}$ which separates the non-faceted–non-faceted (NF–NF) eutectics from faceted–non-faceted (F–NF) eutectics [5]; the volume fraction of the potentially useful ferromagnetic MnSb phase at the eutectic composition is calculated to be about 0.3 from the Sb–Mn binary phase diagram, a critical value determining a lamellar or rod-like eutectic [6]. However, very little has been published on the growth of these kinds of eutectic. The inherent correlations between microstructures, solidification behaviour, crystallographic orientation and magnetic properties of MnSb–Sb eutectic have not been studied systematically to any great extent. The scope of present work therefore is to investigate further the directional solidification, to quantify the microstructures observed and to determine the crystallography and magnetic characterization of the MnSb–Sb eutectic composite.

2. Experimental procedure

Master alloy was first prepared from commercially pure Sb (99.5 wt% or greater) and Mn (99.7 wt% or greater). For the eutectic, the precisely weighed components were sealed in an evacuated (1.33 mPa) quartz tube and melted in a resistance furnace maintained at 1073 K to ensure homogeneity. The directional solidification of the alloy was performed using the Bridgman technique in a high-temperature gradient, G_L, which could be attained to 96–123 $K\,cm^{-1}$ by controlling the furnace temperature and the cooling intensity of the crystallizer.

Directionally solidified samples were sectioned along directions parallel and transverse to the direction of solidification for metallographic examination using standard abrasive polishing techniques. A dilute HCl acid etch was applied to enhance phase contrast. The interrod spacing λ and rod size were measured

over the range of accessible growth velocities (1–25 $\mu m\,s^{-1}$) by statistically determining the rod density, N_r, and rod diameter, d, respectively, in a Reichert MeF3 optical microscope. λ was defined as follows:

$$\lambda = N_r^{-1/2} \quad (1)$$

Thin (about 0.5 mm) slices were cut from the directionally solidified samples both longitudinally and transversely and then ground mechanically down to a thickness of about 0.1 mm. They were further thinned by electrolytic polishing, using the double-jet method, in a bath of KI saturated solution and 2% HCl. Finally, the thin foil was subjected to ion sputtering to obtain a contamination-free surface. The crystallographic orientation was determined by selected area electron diffraction (SAD) on a JEM 2000EX transmission electron microscope operated at 160 kV.

Magnetization measurements were carried out on cylindrically shaped samples at 298 K in an applied field up to $40 \times 10^4\ A\,m^{-1}$ using a vibrating-sample magnetometer. The samples were oriented with the axis along the rod parallel to the field direction.

3. Results and discussion

3.1. Microstructure of MnSb–Sb eutectic

The microstructure of MnSb–Sb eutectic is the idealized structure for the composite *in situ*: an aligned array of metallic MnSb rods (dark grey) embedded in a Sb matrix (white), as shown in Fig. 1. MnSb has straightforwardly grown to long rods along the opposite direction of heat flux during directional solidification at $G_L = 123\ K\,cm^{-1}$ and $V = 2.5\ \mu m\,s^{-1}$; rods are arranged in a regular lattice-like array and are well distributed throughout the transverse section of the sample. To reveal the three-dimensional appearance of the MnSb phase, the Sb matrix in the eutectic solidified at $G_L = 96\ K\,cm^{-1}$ and $V = 2.5\ \mu m\,s^{-1}$ was mechanically stripped. The fibre structure is evident in Fig. 2, which shows a crystalline rod with a parallel array, an average diameter of about 4.5 μm and an interrod spacing of 9.4 μm similar to those in Fig. 1. Attempts were made to confirm the effect of G_L on the spacing. The micrographs of the typical longitudinal sections displayed in Fig. 3 are for two samples with different G_L values but the same V; almost the same configuration exists. Obviously, we can thus argue that G_L plays little role in the spacing selection of the

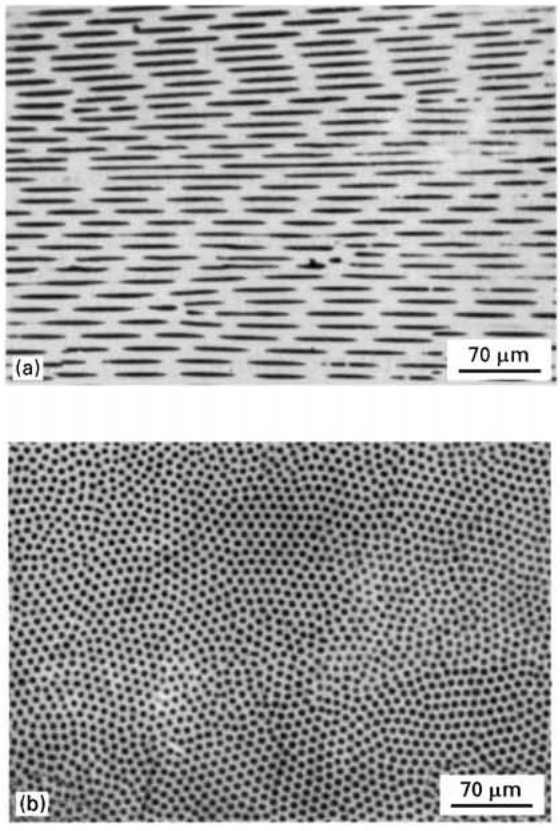

Figure 1 The rod-like morphology of MnSb–Sb eutectic directionally solidified at $G_L = 123\ K\,cm^{-1}$ and $V = 2.5\ \mu m\,s^{-1}$: (a) longitudinal section; (b) transverse section.

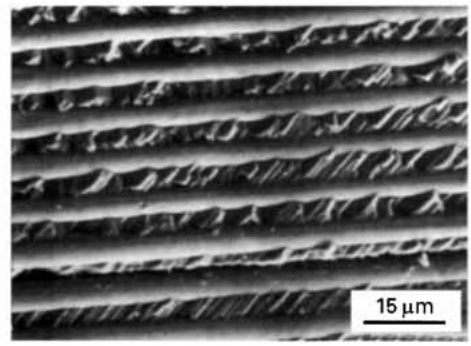

Figure 2 A scanning electron micrograph of MnSb–Sb eutectic after stripping the Sb matrix to reveal MnSb fibres.

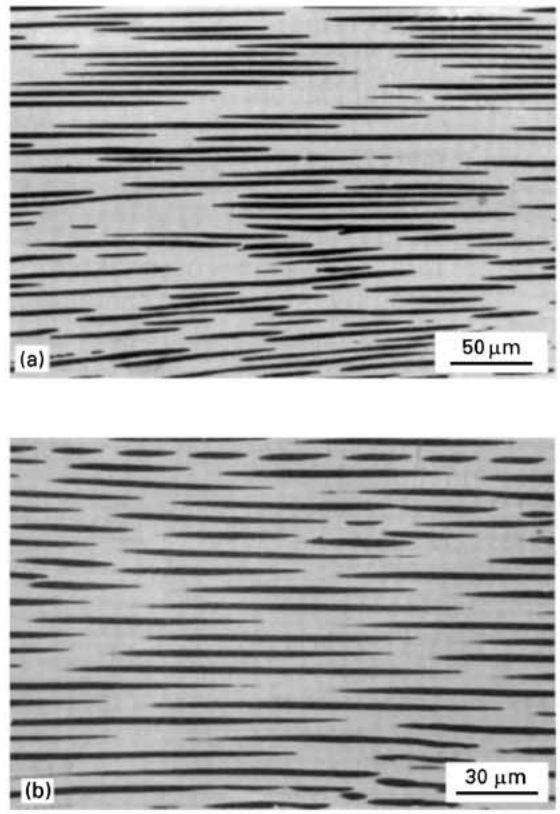

Figure 3 Microstructure of MnSb–Sb composites processed at different G_L with a growth velocity $V = 5\ \mu m\,s^{-1}$: (a) $G_L = 96\ K\,cm^{-1}$; (b) $G_L = 123\ K\,cm^{-1}$.

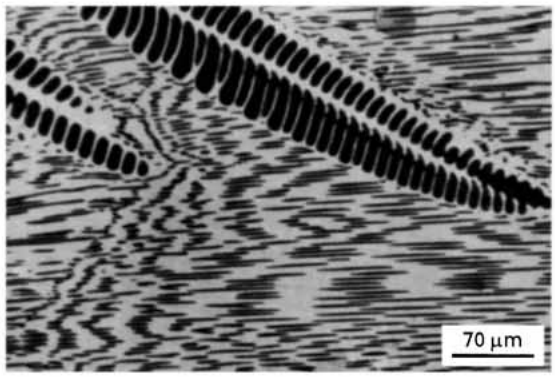

Figure 4 Non-facet characteristic of MnSb.

MnSb–Sb eutectic during directional solidification; this will be further discussed below.

The regularity of the eutectic is believed to be determined by the nature of crystal growth, which has been attracting metallurgists in recent years, especially for eutectic systems with a relatively high entropy of solution. Theoretically, it is possible to determine the non-faceting or faceting tendency of the MnSb phase through entropy-of-solution calculations; yet this is made difficult because of the complicated crystallography of the intermetallic compound. Information on the tendency can, however, be deduced from an examination of the shapes of MnSb primaries in alloys slightly removed from the eutectic composition. Experiments for Sb–9.8 wt % Mn hypereutectic alloy were performed under directional solidification to identify the typical dendrites of MnSb, as shown in Fig. 4. Apparently, the MnSb phase is a non-faceting phase when the composition is close to eutectic. The eutectic matrix may exhibit a non-faceting or weak faceting feature due to ΔS_α near to the critical value presented in the introduction. However, it could be proposed that, since it completely surrounds the rod phase, the matrix must grow with a concave solid–liquid interface around the circumference which provides many re-entrant corners where easy atomic addition can be made from the melt. Faceting of Sb matrix in MnSb–Sb eutectic is believed to be impossible, which determines the eutectic growth in NF–NF type.

The response of λ and d to the growth velocity is studied to confirm the argument concerning the MnSb–Sb eutectic growth pattern. The variation in microstructure with growth velocity is shown in Fig. 5, which displays a significant increase in rod density, but all the MnSb rods are circular in cross-section. Combination of Fig. 1, Fig. 3 and Fig. 5 indicates that the eutectic composite *in situ* may be successfully fabricated for magnetic applications under the present directional solidification conditions.

According to models of eutectic solidification, the relation between λ and V, a scaling law, can be written as the general form

$$\lambda = KV^{-n} \tag{2}$$

where K is a constant for a particular eutectic system. Measurements of λ and d (at three temperature gradients) versus V are plotted in Fig. 6. It is clear that over the investigation range of V, the data are consistent with Equation 2, a linear decrease in λ with increasing V in a dual-logarithmic coordinate; λ varied from 15.1 μm at $V = 1$ μm s^{-1} to 3.4 μm at $V = 25$ μm s^{-1}. Little scatter caused by different G_L is observed. A precise regression is carried out on the available data by computer and this is based on the least-squares fit having the following scaling law for MnSb–Sb eutectic with a correlation coefficient of -0.960:

$$\lambda = 13.9V^{-0.44}\ (\mu\text{m}) \tag{3}$$

It should be pointed out that two important phenomena are summarized from above results.

1. Comparison of Equation 3 with $\lambda^2 V =$ constant given by Jackson and Hunt [7], a model of NF–NF eutectic growth, shows that the exponent (-0.44) derived from the experiments is close to the value of -0.50 predicted by the Jackson–Hunt model.

2. It has been demonstrated that the spacing of the F–NF eutectic is significantly affected by temperature gradient for a given growth velocity [8–10]. However, independence of the spacing with temperature gradient is detected experimentally for MnSb–Sb eutectic.

It is satisfactorily confirmed that the eutectic has a regular NF–NF growth pattern from the two aspects described. As suggested by our previous investigation [11], MnSb–Sb eutectic spacing selection is

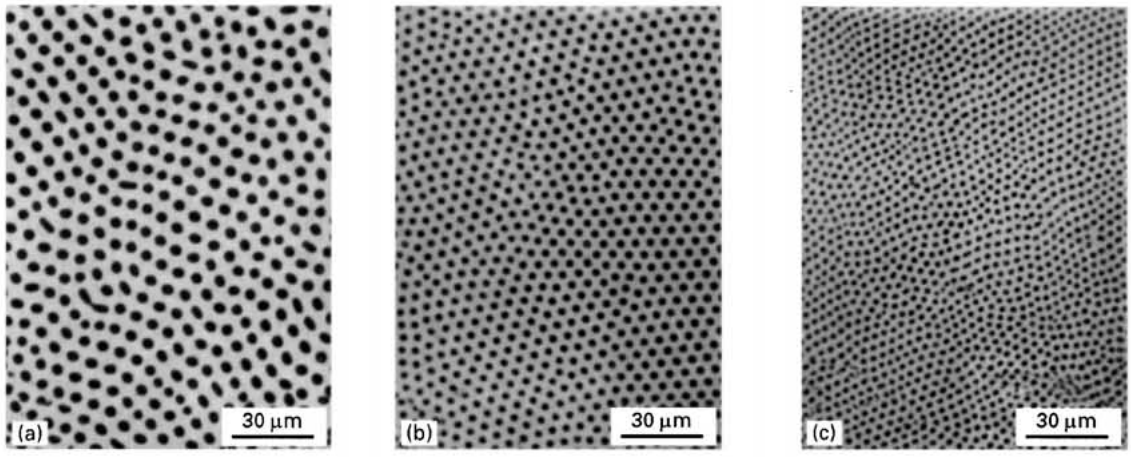

Figure 5 Effect of growth velocity on the eutectic morphology: (a) $V = 2.0$ μm s^{-1}; (b) $V = 8.0$ μm s^{-1}; (c) $V = 15$ μm s^{-1}.

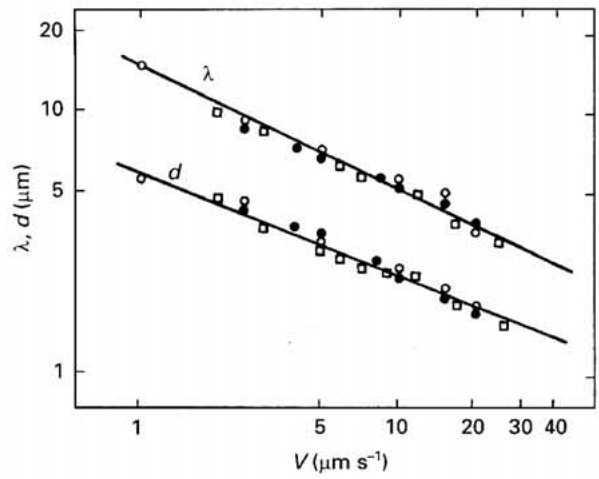

Figure 6 Variation in interrod spacing and rod diameter with growth velocity at different temperature gradients. (○), $G_L = 96\ K\ cm^{-1}$; (□), $G_L = 108\ K\ cm^{-1}$; (●), $G_L = 123\ K\ cm^{-1}$.

recognized to result mainly from the coupling behaviour between the solute diffusion and surface tension with no effect of thermal transfer expressed by G_L, being in agreement with present work.

It also can be found in Fig. 6 that the linear relation between the rod diameter, d, and the growth velocity, V, is similar to those of spacings and V; d varied from 5.7 μm at $V = 1\ \mu m\ s^{-1}$ to 1.5 μm at $V = 25\ \mu m\ s^{-1}$. The regressive formula, with a correlation coefficient of -0.963, is given as follows:

$$d = 6.073V^{-0.41}\ (\mu m) \tag{4}$$

These explanations will not only give rise to a new insight into eutectic growth but also offer a criterion for controlling the microstructure of MnSb–Sb composite.

3.2. Crystallographic orientation of MnSb growth

In the light of the highly anisotropic magnetic properties, crystalline anisotropy (an intrinsic dependence on the crystal growth direction) should play a major role in the composite in addition to shape anisotropy of MnSb rods. It is likely that the superposition of both anisotropies will give the desired properties because of the strong magnetocrystalline anisotropy of MnSb.

Fig. 7 shows the electron diffraction pattern (EDP) of [001] and [011] zone axes of MnSb in the specimen cut transversely from the sample directionally solidified at $G_L = 108\ K\ cm^{-1}$ and $V = 5\ \mu m\ s^{-1}$. The [001] EDP is obtained for the electron beam parallel to the rod axis and the [011] EDP when the specimen is tilted to a certain extent. Evidently, both patterns are concluded to be equivalent results which indicate that

$$[001]_{MnSb}//\text{rod axis}//\text{growth direction} \tag{5}$$

in terms of the crystallography in the hexagonal system. Fig. 7b can be considered to be the result of 35.5° rotation around $[100]^*_{MnSb}$ from Fig. 7a. It should be pointed out that the (110) strong and the (100) and (010) fine spots exist alternately in Fig. 7a, which certainly is evidence of the ordered structure of MnSb

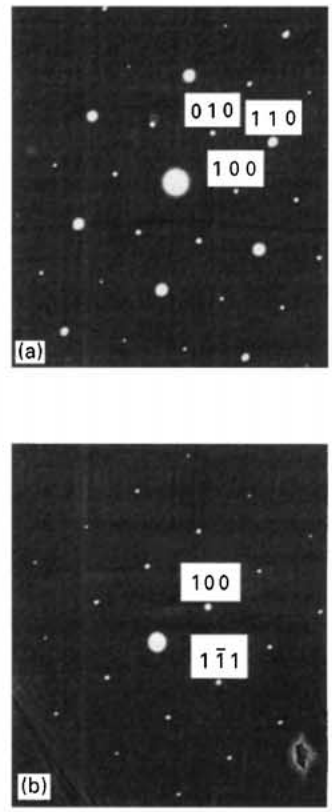

Figure 7 EDPs of MnSb: (a) $\boldsymbol{B} = [001]$; (b) $\boldsymbol{B} = [011]$.

formed upon directional solidification. MnSb has a hexagonal structure ($a = 0.413$ nm; $c = 0.579$ nm) of the NiAs type [3, 12] with the space group, $P6_3/mmc$. Based on positions occupied by Sb and Mn atoms, the structure factor, F_g, for a crystal plane (hkl) can be formulated as follows:

$$F_g = f_{Mn} + f_{Mn}\exp\left(2\pi i\frac{l}{2}\right) + f_{Sb}\exp\left[2\pi i\left(\frac{h}{3}+\frac{2k}{3}+\frac{l}{4}\right)\right] + f_{Sb}\exp\left[2\pi i\left(\frac{2h}{3}+\frac{k}{3}+\frac{3l}{4}\right)\right] \tag{6}$$

where f_{Mn} and f_{Sb} are reflection magnitudes of Mn and Sb atoms, respectively. Equation 6 is simplified to

$$F_g = \begin{cases} 2f_{Mn} - f_{Sb} \\ 2f_{Mn} + 2f_{Sb} \end{cases} \text{for} \begin{cases} (100)\ \text{or}\ (010) \\ (110) \end{cases}$$

Certainly, the diffraction intensity of (110) is higher than those of (100) or (010), which is in complete agreement with the EDP observed in Fig. 7a.

The EDP (Fig. 8) of the [210] zone axis of MnSn fibre was obtained for another specimen cut longitudinally from the sample directionally solidified at $G_L = 108\ K\ cm^{-1}$ and $V = 2\ \mu m\ s^{-1}$ to identify whether the orientation relation (5) is valid for present samples. It should be noted, here, that the specimen observed is carefully regulated to ensure that the rod axis is perpendicular to the electron beam and strictly along the growth direction of the composite. This observation further confirms that the MnSb has grown in the [001] direction as viewed from the crystallography of $[001]_{MnSb} \perp [210]_{MnSb}$. In reality, several MnSb rods in different specimens have been

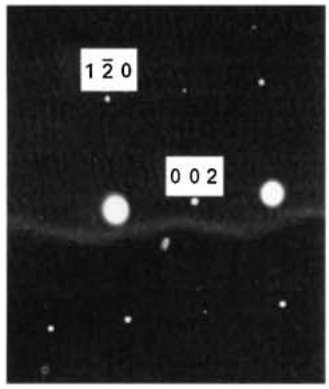

Figure 8 EDP of longitudinally sectioned MnSb.

examined by SAD and most of the rods can be tilted to the orientation given in relation (5).

3.3. Magnetic characterization

The hysteresis loops obtained at room temperature parallel to the growth direction for three directionally solidified composites are shown in Fig. 9, which illustrates the similar dependences of the magnetizations of the samples on the magnetic field applied. All loops consist of two very close curves, termed the narrow loops, exhibiting very low magnetic remanence and intrinsic coercivity. It is important to note that the saturation magnetization, σ_s, increases from 26.3 A m^2 kg^{-1} at $\lambda = 9.1$ μm and $d = 4.5$ μm to 30.2 A m^2 kg^{-1} at $\lambda = 5.5$ μm and $d = 2.6$ μm, resulting from an increase in V from 2.5 to 10 μm s^{-1}. However, σ_s did not increase further for the sample directionally solidified at a higher growth velocity $V = 15$ μm s^{-1} even though both λ and d decrease to 4.9 μm and 2.1 μm, respectively. This may be a consequence of the formation of a cellular eutectic structure in which MnSb rods were out of highly parallel alignment, and thus any enhancement of magnetization due to shape anisotropy would be ensured besides the size reduction of MnSb. The maximum magnetization obtained in the composites can be converted to a value $\sigma_s = 100.7$ A m^2 kg^{-1} for MnSb rods, not including the contribution from the diamagnetic Sb matrix (70% by volume), which is in agreement with previous work of $\sigma_s = 102.5$ A m^2 kg^{-1} at 300 K [2]. Fig. 9 displays the constant permeability over the wide field range 0–240 000 A m^{-1} at growth velocities of 2.5 and 10 μm s^{-1}, which is known to be dependent on magnetic domain rotation. It shows that the easy axis of magnetization in MnSb, with a Curie temperature of 588 K, lay in the c plane at room temperature; above 520 K the easy axis was along the c axis [12]. According to the above crystallographic demonstration, $[001]_{MnSb}$ in the cylindrical samples oriented along the field direction implies that the magnetization is along the hard axis. In this case, the domain rotation mechanism dominates the constant permeability of the composite. As shown in Fig. 9, there is a clear reduction in the field range (0–160 000 A m^{-1}) when maintaining the constant permeability for the composite solidified at $V = 15$ μm s^{-1}. This phenomenon may be explained by the deviation of [001] of partial MnSb rods from the growth direction, corresponding to the cellular eutectic formed.

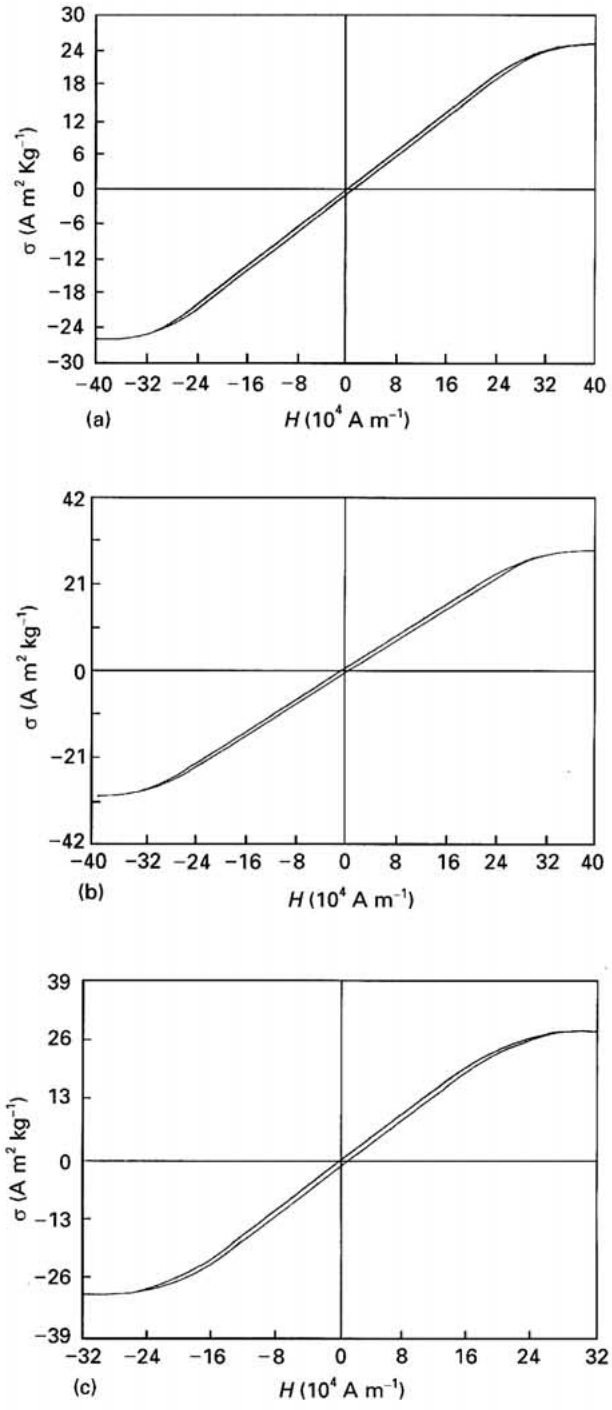

Figure 9 Hysteresis loops of directionally solidified MnSb–Sb composites: (a) $V = 2.5$ μm s^{-1}; (b) $V = 10$ μm s^{-1}; (c) $V = 15$ μm s^{-1}.

4. Conclusion

MnSb–Sb eutectic composite, containing ferromagnetic MnSb rods preferentially along the growth direction, has been produced by directional solidification. MnSb–Sb eutectic is characterized by NF–NF type growth and a well-distributed fibre microstructure even though Sb–Mn alloy is a unique system with a high entropy of solution. The measurements have shown that the interrod spacing, λ, and rod diameter,

d, are independent of temperature gradient, G_L. The scaling laws of variation in λ (or d) with growth velocity, V, are developed in the light of the eutectic solidified at various growth conditions of $G_L = 96$, 108 and 123 K cm^{-1}, $V = 1$–25 μm s^{-1}, i.e. $\lambda = 13.9\,V^{-0.44}$ and $d = 6.073V^{-0.41}$ (μm). The crystal orientation of MnSb rods is approached by means of electron diffraction, which reveals that the MnSb rods, with a hexagonal NiAs-type ordered structure, grew in the [001] direction. The following orientation relation exists:

$$[001]_{MnSb}//\text{rod axis}//\text{growth direction}$$

The hysteresis loops of the MnSb–Sb eutectic composite, exhibiting a very low magnetic remanence and instrinsic coercivity, are determined. The saturation magnetization, σ_s, increases with reducing dimensions, λ and d, of MnSb, but no continuous enhancement occurs when the cellular eutectic structure forms. Constant permeability over a wide range of magnetic fields has been realized with $[001]_{MnSb}$ parallel with the field direction, which is related to domain rotation.

Acknowledgements

The authors would like to thank Professor G. J. Shen and Professor S. D. Wang of Southeast University for their help with the crystallographic determination, and Professor J. W. Zhao and Professor G. Q. Wang of Nanjing University for helpful discussions concerning the magnetic properties. Financial support from the Doctoral Foundation of State Education Commission of China and the Scientific Research Foundation of Science and Technology Committee of Jiangsu Province are acknowledged.

References

1. W. ALLEN and W. STUTIUS, *Solid State Commun.* **20** (1976) 561.
2. G. MARKANDEYULU and K. V. S. RAMA RAO, *J. Magn. Magn. Mater.* **67** (1987) 215.
3. C. V. NARASIMHA, S. L. PINJARE and K. V. S. RAMA RAO, *ibid.* **50** (1985) 107.
4. T. OKITA and Y. MAKINO, *J. Phys. Soc. Jpn* **259** (1968) 120.
5. M. N. CROKER, R. S. FIDLER and R. W. SMITH, *Proc. R. Soc. A* **335** (1973) 15.
6. R. ELLIOT, "Eutectic solidification processing: crystalline and glassy alloys" (Butterworth, London, 1983) p. 107.
7. K. A. JACKSON and J. D. HUNT, *Trans. AIME* **236** (1966) 1129.
8. D. J. FISHER and W. KURZ, *Acta Metall.* **28** (1980) 777.
9. J. M. LIU, Y. H. ZHOU and B. L. SHANG, *Acta Metall. Mater.* **38** (1990) 1631.
10. P. MAGIN, J. T. MASON and R. TRIVEDI, *ibid.* **39** (1991) 469.
11. Y. PAN and G. X. SUN, *Acta Metall. Sin.* **32** (1996) 120.
12. W. J. TAKEI, D. E. COX and G. SHIRANE, *Phys. Rev.* **129** (1963) 2008.

Received 2 July
and accepted 19 December 1996